Ab initio thermal rate calculations of HO + HO = O(3P) + H 2O reaction and isotopologues

ARTICLE *in* THE JOURNAL OF PHYSICAL CHEMISTRY A · MARCH 2013

Impact Factor: 2.69 · DOI: 10.1021/jp312246q · Source: PubMed

2 AUTHORS:

Thanh Lam Nguyen
University of Texas at Austin
72 PUBLICATIONS **1,382** CITATIONS
SEE PROFILE

John F Stanton
University of Texas at Austin
5 PUBLICATIONS **75** CITATIONS
SEE PROFILE

THE JOURNAL OF PHYSICAL CHEMISTRY A

Article

pubs.acs.org/JPCA

Ab Initio Thermal Rate Calculations of HO + HO = O(^{3}P) + H_2O Reaction and Isotopologues

Thanh Lam Nguyen and John F. Stanton*

Department of Chemistry & Biochemistry, The University of Texas at Austin, Texas 78712-0165, United States

Supporting Information

ABSTRACT: The forward and reverse reactions, HO + HO ⇌ O(^{3}P) + H_2O, which play roles in both combustion and laboratory studies, were theoretically characterized with a master equation approach to compute thermal reaction rate constants at both the low and high pressure limits. Our ab initio $k(T)$ results for the title reaction and two isotopic variants agree very well with experiments (within 15%) over a wide temperature range. The calculated reaction rate shows a distinctly non-Arrhenius behavior and a strong curvature consistent with the experiment. This characteristic behavior is due to effects of positive barrier height and quantum mechanical tunneling. Tunneling is very important and contributes more than 70% of total reaction rate at room temperature. A prereactive complex is also important in the overall reaction scheme.

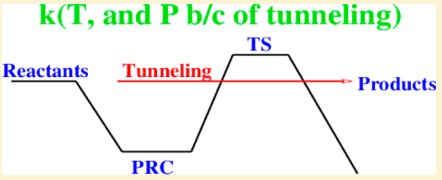

INTRODUCTION

The self-reaction of hydroxyl radicals can proceed through two primary, distinctive product pathways R1 and R2:

$$HO + HO = O(^3P) + H_2O \quad (R1)$$

$$HO + HO + [M] = H_2O_2 + [M] \quad (R2)$$

Reaction R2 occurring on the singlet electronic state potential energy surface (PES) is obviously pressure dependent,[1−3] whereas the rate of reaction R1 on multiple triplet electronic state PESs is generally assumed to be pressure independent.[4] Our interest is to focus on the forward R1 and reverse R-1 reaction, the latter of which is of considerable importance in combustion (e.g., in hydrocarbon and hydrogen flame).[5,6]

$$O(^3P) + H_2O = HO + HO \quad (R\text{-}1)$$

The forward reaction R1 is essentially a chain-terminating step, thus inhibiting the combustion process. In contrast, the reverse reaction R-1 is a chain-propagating step, so it accelerates flame propagation.[5,6] Because OH concentrations in the atmosphere are low, the self-reaction R1 is negligible. Unlike in the atmosphere, however, the disproportionation reaction of HO radicals is frequently important in laboratory studies when HO radicals are produced with high concentrations, such as, for example, study of HO-initiated oxidations of chemical compounds.[4,7,8]

Because of its importance, the title reaction has been an object of numerous experimental and theoretical studies. Two excellent reviews can be found in the recent work of Bahng et al.[8] and of Sangwan et al.[4] The thermal rate constants of the title reaction were reviewed and evaluated a few times.[9,10] On the experimental side,[4,7−16] the thermal reaction rates measured as a function of temperature show a non-Arrhenius behavior and a strong curvature, e.g., negative temperature-dependence at low temperatures and positive temperature-dependence at high temperatures. As a result, the thermal rate constant appears to have a minimum at about 400 to 500 K.[4,9] This observation is very unusual given that all previous theoretical calculations provided positive barriers for the H-abstraction of the title reaction. In addition, at around room temperature there is a large scatter, by a factor of about 2, for thermal reaction rates measured by various groups.[7,8,14] In 1999, Bedjanian et al.[7] found a room temperature rate constant of $(1.40 \pm 0.19) \times 10^{-12}$ cm^3 molecule^{-1} s^{-1} using the mass spectrometric discharge-flow method. Eight years later, Bahng and Macdonald[8] detected a higher value of $(2.7 \pm 0.9) \times 10^{-12}$ cm^3 molecule^{-1} s^{-1} via direct concentration measurements of the OH radical using high-resolution diode laser absorption spectroscopy. Very recently, Sangwan et al.[4] remeasured thermal rate constants of the title reaction at moderate temperature range (555 to 834 K) using the pulsed laser photolysis coupled to transient UV−vis absorption spectroscopy. The observed results by these workers appear consistent with the group of low values of Bedjanian (see Figure 4 below). Bedjanian et al.[7] also studied kinetically two isotopic reactions R3 and R4:

$$HO + DO = O(^3P) + HOD \quad (R3)$$

$$DO + DO = O(^3P) + D_2O \quad (R4)$$

At room temperature, they observed thermal rates of $(1.51 \pm 0.27) \times 10^{-12}$ cm^3 molecule^{-1} s^{-1} and $(4.34 \pm 0.63) \times 10^{-13}$ cm^3 molecule^{-1} s^{-1} for reactions R3 and R4, respectively.[7] Ideally, the sum $k_1 + k_4$ should be about twice as fast as k_3 (see ref 7). However, this condition is not met by the experiments of Bedjanian et al.[7] for an unknown reason. Using k_3 and k_4 of

Received: December 12, 2012
Revised: March 7, 2013

   dx.doi.org/10.1021/jp312246q | J. Phys. Chem. A XXXX, XXX, XXX−XXX

Bedjanian et al., k_1 at 298 K is estimated to be ca. $(2.6 \pm 0.5) \times 10^{-12}$ cm^3 molecule^{-1} s^{-1}, which is ca. two times larger than the value of Bedjanian et al., but in excellent agreement with that measured by Bahng and Macdonald.[8] (Our results obtained from first-principles calculations in this work also support the high values for thermal rate constants). On the theoretical side,[17−19] the lowest- and higher-lying triplet electronic state potential energy surfaces for the title reaction were calculated using various levels of theory.[17−19] Global potential energy surfaces for the reserve reaction constructed using the CASSCF +MP2 method are also available.[19] Thermal rate constants were computed using the improved variational transition state theory (ICVT) corrected for tunneling with a small curvature semiclassical adiabatic ground state (SCSAG) transmission coefficient.[17] The ICVT/SCSAG rate constants were in close agreement with experiments provided that the calculated barrier heights with the MCSSCF and GVB+1+2 method were adjusted by ca. 5 kcal/mol.[17]

Because of the important roles of the title reaction in combustion and laboratory studies, we set out to reinvestigate reaction mechanism and kinetics using highly accurate levels of theory: the HEAT protocol[20−22] and chemical kinetics treatments based on semiclassical transition state theory (SCTST).[23−26] There are three main goals of this work, namely, (i) first, to test the performance of theory versus experiment by comparing ab initio reaction rate constants with experiment; (ii) second, to understand the aforementioned unusual behavior of the thermal rate constant; and finally, (iii) to investigate the possible role of a prereactive complex (PRC), which can enhance the thermal reaction rate constant owing to tunneling and might cause reaction rate constants to be slightly pressure dependent.

COMPUTATIONAL APPROACH

Quantum Chemical Calculations. An interaction of two OH($^2\Pi$) radicals can proceed on four singlet and four triplet electronic state PESs.[22] Our interest in this work is to study the forward and reverse reactions R1 and R-1, which take place on triplet electronic state PESs. All stationary points including minima and transition structures on the two lowest-lying triplet electronic state PESs were computed using the HEAT protocol (see Figure 1).[20−22] The other two higher-lying triplet PESs are highly repulsive, lie very high in energy,[19] and therefore play a negligible role in the temperature range of 200 to 2500 K and are not considered in this work. The HEAT model chemistry includes a treatment of electron correlation that includes quadruple excitations (the variant used here is HEAT-345(Q)) and does not contain any empiricism apart from that associated with basis set extrapolation techniques. In addition to the vibrational zero-point energy, other small adjustments such as scalar relativistic correction, first-order spin−orbit coupling, and the diagonal Born−Oppenheimer correction are included. For an elaborated discussion of the HEAT protocol and the accuracy that has been obtained by this procedure for thermochemical parameters, the interested reader is referred to refs 20−22. For minima on the potential energy surface, HEAT generally provides relative energies (i.e., reaction enthalpy, dissociation energy, and so on) that have proven to have an accuracy of better than 0.24 kcal/mol (1 kJ/mol). For the reaction R1 in particular, HEAT gives a reaction enthalpy of −15.78 kcal/mol at 0 K, which is in excellent agreement with −15.91 ± 0.10 kcal/mol derived from the Active Thermochemical Tables (ATcT).[27] For transition states where the single-reference approach is still adequate (as in the case here), a similar accuracy is expected. Unlike in the original papers, in this work we use zero-point anharmonic vibration energies (ZPE) obtained with CCSD(T) (in the frozen core approximation) in combination with the atomic natural orbital (ANO) basis set of Almlof and Taylor.[28,29] A truncated ANO basis set, here referred to as ANO1, with the truncation 4s2p1d for H atom and 4s3p2d1f for O atom, was used to obtain the anharmonic force fields. The harmonic force fields were computed with ANO2 basis set, which is contracted as 4s3p2d1f for H atom and 5s4p3d2f1g for O atom. Second-order vibrational perturbation theory (VPT2) was then used to compute the zero-point energy. The CFOUR program package was used for all calculations.[30]

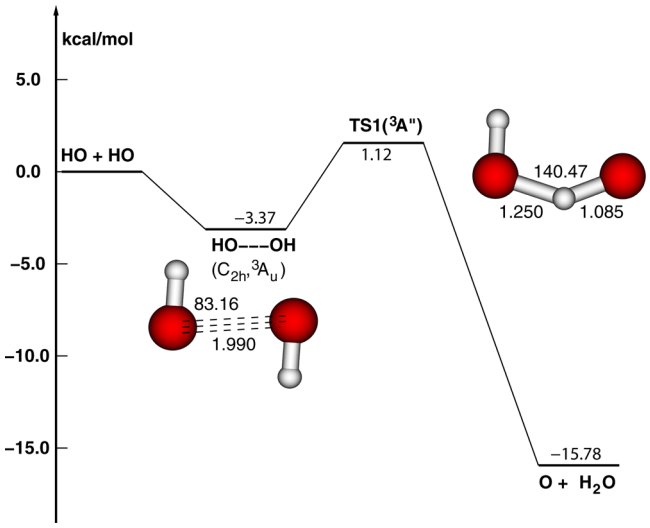

Figure 1. Key stationary points on the lowest-lying triplet state potential energy surface (in kcal/mol) for the HO + HO = O(^{3}P) + H_2O reaction calculated using HEAT protocol (see text). Bond lengths are given in Angstrom, while angles are in degrees.

Chemical Kinetics Calculations. The general reaction scheme of the title reaction (formation of a PRC with subsequent abstraction), as presented in Figure 1, is ubiquitous in atmosphere and combustion chemistry,[9,10,31] for example, the oxidations of organic compounds by hydroxyl radicals. So, it is useful to discuss various available chemical kinetic models, which have been used for the treatments of such reactions. If the reaction R1 did not proceed through a prereactive complex (i.e., the direct H-abstraction mechanism was assumed), the reaction rate constant would undoubtedly be pressure independent. So, transition state theory (TST) approach would be sufficient. With the existence of a PRC, however, the title reaction might depend on pressure. To compute thermal rate constants as functions of both temperature and pressure (i.e., falloff curve), one must use the master equation technique.[32] However, an accurate solution of the two-dimensional master equation for the falloff curve is impractical at this time because an appropriate function of energy transfer depending on both energy and angular momentum is unknown for most reactions. In this work, we focus on the zero-pressure limit, which is relevant to this particular reaction system and straightforward to compute. Therefore, the complicated effects of energy transfer by collisions with a third body are completely neglected. It should be noted here that most experimental work, except that of Sangwan et al.,[4] were studied at low pressures ($P \leq 1$ atm)[7−11,14] where the solution at the low P

dx.doi.org/10.1021/jp312246q | J. Phys. Chem. A XXXX, XXX, XXX−XXX

limit given below is an appropriate point of comparison. An analytical solution of the two-dimensional master equation (i.e., depending on both energy and overall rotation) for thermal rate constants under the low P limit for a reaction scheme as shown in Figure 1 is given by[33−36]

$$k_{P=0}(T) = \frac{1}{h} \times \frac{Q^{\neq}_{\text{trans,elec}}}{Q_{\text{HO}}{}^{2}} \times \sum_{J=0}^{+\infty} (2J+1) \int_{0}^{+\infty} \frac{G_0^{\neq}(E,J) \times G_1^{\neq}(E,J)}{G_0^{\neq}(E,J) + G_1^{\neq}(E,J)} \exp\left(-\frac{E}{k_B T}\right) \mathrm{d}E \quad (1)$$

where h is Planck's constant, k_B is Boltzmann's constant, and Q_{HO} is total partition function of HO. The electronic partition function of HO is given by $Q^{\text{elec}}_{HO} = 2 + 2\exp(-139\ \text{cm}^{-1}/k_B T)$. $Q^{\neq}_{\text{trans,elec}}$ is a product of translational and electronic partition functions corresponding to the transition structure, TS1. $G_1^{\neq}(E,J)$ is the rovibrational cumulative reaction probability (CRP) at each pair of (E,J) for TS1. $G_0^{\neq}(E,J)$ is a rovibrational sum of states for the kinetic bottleneck for the PRC → HO + HO step, which can be computed as a minimum of chemical reaction fluxes passing through the dividing surface using microvariational TST.[37,38] In this work, vibration and rotation are assumed to be separable, so $G(E,J)$ can be computed by convolution and is expressed as

$$G(E,J) = \int_0^E G_{\text{vib}}(E - E_{\text{rot}}) \rho_{\text{rot}}(E_{\text{rot}}) \mathrm{d}E_{\text{rot}} \quad (2)$$

Here, the vibrational CRP for TS1, $G_1^{TS1}(E)$, is calculated using SCTST,[23−26] which includes fully coupled vibrations and multidimensional tunneling, while the vibrational sum of states for variational TS0 is calculated using the BSSR algorithm.[39,40] Rotational energy levels of a rigid symmetric top molecule are used for the transition states, given by $E_{\text{rot}} = \overline{B}J(J+1) + (A - \overline{B})K^2$ with $\overline{B} = (B \times C)^{1/2}$ and $-J \le K \le J$. Both the CRP and the rotational density of states are obtained by explicit state counting, using an energy bin of 1 cm^{-1}, a maximum J of 200, and a ceiling energy of 5×10^4 cm^{-1} relative to the initial reactants. The latter two are chosen to be sufficiently high to ensure that all reaction rates computed in the temperature range from 200 to 2500 K are converged. Equation 1 is computed by simple summation using step sizes of 1 cm^{-1} and unity for E and J, respectively. It should be mentioned that the reaction path degeneracies of 2 and 1 for the PRC → TS1 → $O(^3P)$ + H_2O step and the PRC → variational TS0 → HO + HO step, respectively, are also included into G_1 and G_0. Effects of rovibrational coupling in the partition function of OH were investigated but found to be negligible at the temperature studied.

When G_0 is much larger than G_1 at all energies (i.e., the redissociation of PRC regenerating the initial reactants occurs much more rapidly than the decomposition of PRC leading to the products), eq 1 reduces to eq 3:

$$k_{P=0}(T) = \frac{1}{h} \times \frac{Q^{\neq}_{\text{trans,elec}}}{Q_{\text{HO}}{}^{2}} \times \sum_{J=0}^{+\infty} (2J+1) \int_{0}^{+\infty} G_{\text{TS1}}^{\neq}(E,J) \exp\left(-\frac{E}{k_B T}\right) \mathrm{d}E \quad (3)$$

Equation 3 becomes increasingly more accurate as the barrier for the H-abstraction step via TS1 increases. It is of interest to note that eq 3 is the same formula as the microcanonical version of TST (μTST).[41] The difference between eq 3 and μTST is decided by how $G_1^{\neq}(E,J)$ is computed. In eq 3, $G_1^{\neq}(E,J)$ is computed for the PRC → TS1 → $O(^3P)$ + H_2O path, while with μTST, $G_1^{\neq}(E,J)$ is computed for the HO + HO → TS1 → $O(^3P)$ + H_2O path. Therefore, at lower temperatures, the difference is mainly due to the tunneling correction included into $G_1^{\neq}(E,J)$ because the PESs of two reaction paths are different. $k_{P=0}(T)$ calculated using eq 3 is larger than that of μTST because the PES of the former is narrower, thus the tunneling correction is larger. When tunneling is excluded, eq 3 becomes equivalent to μTST.

As can be seen from eq 3, $k_{P=0}(T)$ depends on TS1 only and is very straightforward to compute. Equation 3 is hereafter designated as the one-TS model. For the title reaction, the thermal rate constants calculated using the one-TS model are slightly overestimated, by less than 15%, as compared to those of the two-TS model, eq 1.

To check whether or not the rate of reaction R1 depends on pressure, thermal rate constants producing the final products ($O(^3P)$ + H_2O) under the high-P limit are also computed using[35,42,43]

$$k_{P=\infty}(T) = k_0(T) \times \frac{k_1(T)}{k_{-0}(T) + k_1(T)} \quad (4)$$

where $k_0(T)$ and $k_{-0}(T)$ are thermal rate constants of the bimolecular association and redissociation reactions, HO + HO ⇌ PRC, respectively; and $k_1(T)$ is a thermal rate constant of the unimolecular decomposition reaction of PRC → $O(^3P)$ + H_2O. The ratio of $(k_1(T))/(k_{-0}(T) + k_1(T))$ corresponds to the fraction of PRC leading to the products under the condition of the thermal equilibrium. Because the prereactive complex stays in a shallow well and has a very short lifetime (on the order of a pico-second), the thermal stabilization of PRC can only occur under the extreme conditions of very low temperature and extremely high pressure. As a result, eq 4 is not likely to be a particularly useful model for practical applications to reactions occurring in the gas phase, such as in the atmosphere and combustion. In contrast, the thermal equilibrium is easy to be achieved for reactions in the solution.

If $k_{-0}(T)$ is much larger than $k_1(T)$ at all temperatures, eq 4 simplifies to eq 5:

$$k_{P=\infty}(T) = k_0(T) \times \frac{k_1(T)}{k_{-0}(T)} = K_{\text{eq}}(T) \times k_1(T) \quad (5)$$

where K_{eq} is the equilibrium constant for the HO + HO ⇌ PRC step.

This assumption is likely to be appropriate because the kinetic bottleneck TS0 is much looser than TS1 and lies lower in energy. Equations 4 and 5 were suggested for the first time in 1976 by Singleton and Cvetanovic. Recently, eq 5 has been widely applied to compute thermal rate constants for reactions in the gas phase,[43] which have a similar reaction scheme to that shown in Figure 1. Although there is a lack of a solid physical foundation, eq 5 is commonly used because of its simplicity.

To have a compete comparison of different formulas at the low-P limit versus the high-P limit, eq 5 is rewritten in terms of the microcanonical form and expressed as eq 5b:

dx.doi.org/10.1021/jp312246q | J. Phys. Chem. A XXXX, XXX, XXX−XXX

Table 1. Calculated Relative Energies (kcal/mol) for Various Species in the HO + HO → O(^{3}P) + H_2O Reaction; Data in Literatures Are Given for the Purpose of Comparison

species	HEAT[a]	Harding and Wagner (1988)	Karkach and Osherov (1999)	Conforti et al. (2010)[b]	ATcT[c]
HO + HO	0.00 (0.00)	0.0	0.00	0.0	0.0
O(^{3}P) + H_2O	−15.78	N/A	−15.77	−14.1	−15.91 ± 0.10
PRC(C_{2h}, ^3A_u)	−3.37	∼−4.3	−3.73	N/A	N/A
TS1(C_s, $^3A''$)	+1.12 (+1.28)	+7.7	+1.61	+1.8	N/A
TS2(C_s, $^3A'$)	+5.89	+10.1	N/A	+8.8	N/A

[a]The values in parentheses are calculated with the HEAT protocol using the ROHF reference, while the others are based on the UHF reference. [b]From the fitted PES, which was constructed using the CASSCF+MP2 method. [c]Heats of formation at 0 K for various species were taken from the Active Thermochemical Tables (ref 27), including $\Delta H^0_f(OH)$ = 8.867 ± 0.072 kcal/mol, $\Delta H^0_f(H_2O)$ = −57.104 ± 0.010 kcal/mol, and $\Delta H^0_f(O)$ = 58.985 ± 0.024 kcal/mol.

$$k_{P=\infty}(T) = \frac{1}{h} \times \frac{Q^{\neq}_{\text{trans,elec}}}{Q_{\text{HO}}^{\,2}} \times \sum_{J=0}^{+\infty} (2J+1) \int_{\Delta E_0}^{+\infty} G^{\neq}_{\text{TS1}}(E, J) \exp\left(-\frac{E}{k_B T}\right) dE \quad (5b)$$

Equation 5b for the high-P limit looks very similar to eq 3 for the low-P limit. The difference lies at the lower limit of the integrals. At the low-P limit, the lower limit of integral is at the energy level of the initial reactants (HO + HO), whereas at the high-P limit, the integral starts from the lower energy level of the prereactive complex, PRC. By splitting the integral of eq 5b into two regions, above and below the reactants, eq 5b can then be rearranged to eq 5c:

$$k_{P=\infty}(T) = k_{P=0}(T) + \Delta k \quad (5c)$$

in which Δk (always ≥ 0) is the difference between $k_{P=\infty}(T)$ and $k_{P=0}(T)$ and is given by eq 6:

$$\Delta k = \frac{1}{h} \times \frac{Q^{\neq}_{\text{trans,elec}}}{Q_{\text{HO}}^{\,2}} \times \sum_{J=0}^{+\infty} (2J+1) \int_{\Delta E_0}^{0} G^{\neq}_{\text{TS1}}(E, J) \exp\left(-\frac{E}{k_B T}\right) dE \quad (6)$$

Equation 6 presents the integral to be calculated from the energy level of PRC to that of the initial reactants. This is a classically forbidden region leading to the products via TS1. Therefore, it can be said that eq 6 corresponds to an additional contribution of quantum mechanical effects in the classical-forbidden region to thermal rate constant under the conditions of the high-P limit. Equation 6 will be called the tunneling rate constant at the high-P limit. Without tunneling, Δk is of course equal to zero; thus, $k_{P=\infty}(T)$ equals $k_{P=0}(T)$. In other words, the reaction becomes necessarily pressure independent when quantum mechanical tunneling is not included. It is well-known that the quantum mechanical tunneling plays its most important role at low temperatures, which are relevant to reactions in the atmosphere, but is very minor at the high temperatures characteristic of combustion. Thus, the difference between the two kinetic models at the high- and low-P limits is a low temperature effect, which becomes negligibly small at high temperatures. In general, the kinetic model at the high-P limit always overestimates reaction rate constants. From this analysis, we recommend that either eq 1 or eq 3 should be used in place of the common eq 5 for the purpose of atmospheric applications.

RESULTS AND DISCUSSION

Potential Energy Surfaces. Triplet state potential energy surfaces of the title reaction is presented in Figure 1, while relative energies of various species are tabulated in Table 1. As can be seen, we are able to reproduce the ATcT reaction enthalpy,[27] within 0.1 kcal/mol, using the HEAT protocol. To the best of our knowledge, the HEAT protocol is the highest level of theory that has been applied to this reaction until now. Of the three other methods in Table 1, the values obtained with the G2(QCI)-like method by Karkach and Osherov[18] are in very good agreement with the HEAT, within 0.5 kcal/mol. The fitted PES, which was constructed using the CASSCF+MP2 method by Conforti et al.,[19] is in slightly less good agreement; its values are about 1−3 kcal/mol higher than the HEAT. Finally, the early calculations of Harding and Wagner[17] overestimate the HEAT by about 5−6 kcal/mol. These workers[17] made a comparable adjustment to the barrier to bring the calculated reaction rate constant into agreement with experiment at 298 K.

Figure 1 shows that the first step in the self-reaction of two HO radicals on the lowest-lying triplet state PES is to form a prereactive complex (PRC), which lies about 3.4 kcal/mol lower in energy than the asymptotic reactants. The binding energy of the PRC is due to a combination of two hydrogen bonds and dipole interactions. The PRC has a C_{2h} symmetry and a ^3A_u electronic state, in which one unpaired electron is in a B_g orbital and the other is in a B_u orbital (see Figure S1 in Supporting Information). The vibrationally excited, nascent PRC when it is formed can then either redissociate back to the initial reactants or proceed by H-abstraction via TS1 leading to the products, O(^{3}P) + H_2O. Therefore, the formation of products depends on the competition of these two reaction pathways. This competition is formulated in eq 1. Generally, the first step has a lower barrier and is more entropic favored (i.e., with a looser TS) than the latter, so the redissociation is expected to be much faster. In contrast, the H-abstraction step has some contributions from tunneling, so it may become important at low temperatures. In addition, at high pressures, some fraction of energized PRC (without additional energy) will lose its internal energy by collisions and cannot proceed to redissociate but can carry out the H-abstraction to the products via tunneling, resulting in an increase of the product formation reaction rate constant. As a result, because of tunneling, the reaction rate might depend on pressure.

In TS1, the breaking O−H bond length is elongated by 0.11 Å, while the forming O−H bond has a length of 1.25 Å. So, TS1 is an early transition structure with a barrier of +1.12 kcal/mol relative to the reactants. This value was calculated with the HEAT protocol using the unrestricted Hartree−Fock (UHF)

dx.doi.org/10.1021/jp312246q | J. Phys. Chem. A XXXX, XXX, XXX−XXX

reference, which has the expectation value of $\langle S^2 \rangle = 2.045$. It is well established that the thermal rate constant depends sensitively on the calculated barrier. To check the effects of the HF reference and spin-contamination on the barrier, we reran the HEAT calculations using the restricted open-shell Hartree–Fock (ROHF) reference (which involves slightly different geometries). We obtained a barrier of +1.28 kcal/mol with the ROHF reference, which is only 0.16 kcal/mol higher than the UHF reference. This difference is due to the truncation of the full-CI method that is used in the HEAT. Taking an average of these values, we obtain 1.20 ± 0.10 kcal/mol for the calculated barrier. This value will be used for chemical kinetics calculations later.

We are able to locate another transition state, TS2, having a $^3A'$ state (not shown in Figure 1; see Figure S2 in the Supporting Information). TS2 is the first excited electronic state of TS1, and it lies about 5.9 kcal/mol above the initial reactants. As a result, TS2 may play some roles at high temperatures although its contribution at low temperatures is negligibly small. However, the analysis of harmonic vibrational frequencies then shows that TS2 is a second-order saddle point. So, TS2 will not be included into the following chemical kinetics calculations. Because of this simplification, our calculated thermal rate constants in this work might be slightly lower than the actual values under the conditions characteristic of combustion.

Thermal Rate Constants. The calculated thermal rate constants as functions of temperatures for three reactions R3, R4, and R1 are shown in Figures 2, 3, and 4, respectively. The

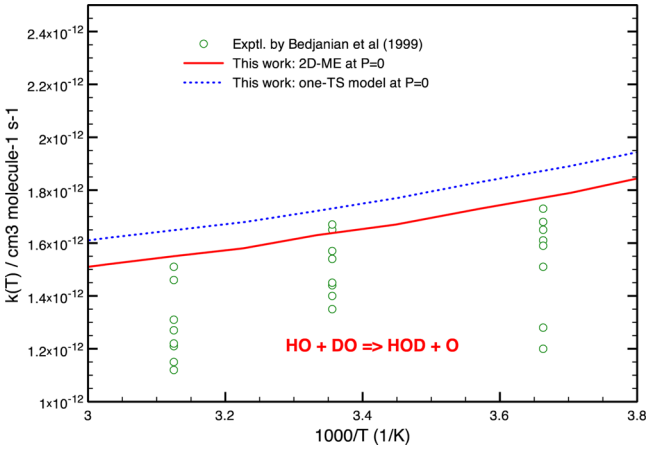

Figure 2. Calculated thermal rate constants as a function of temperature for the HO + DO = $O(^3P)$ + HOD reaction.

data reported in the literature are also included for the purpose of comparison. The two reactions R3 and R4 are selected to be discussed first because their results are used to understand a difference between some experiments and the theory for the reaction R1, which is shown in Figure 4. Figures 2 and 3 show that the calculated reaction rate constants for the isotopic reactions using two-TS model (i.e., eq 1) agree reasonably well with the experiments of Bedjanian et al.,[7] within 15%, in the temperature range of 250 to 360 K. For the reaction HO + DO, the trend of negative temperature dependence for $k(T)$ is also reproduced by the theory, whereas there is a qualitative (but small in magnitude) difference for the reaction DO + DO. The differences between the HO + DO and DO + DO cases are determined by two things, namely, (i) first, the barrier of 1.59

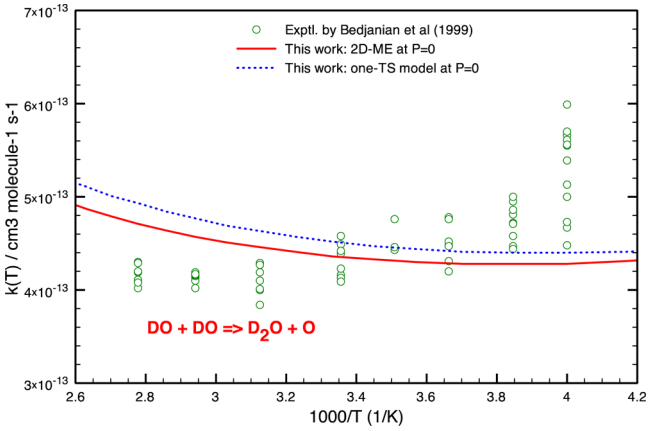

Figure 3. Calculated reaction rate constants as a function of temperature for the DO + DO = $O(^3P)$ + D_2O reaction.

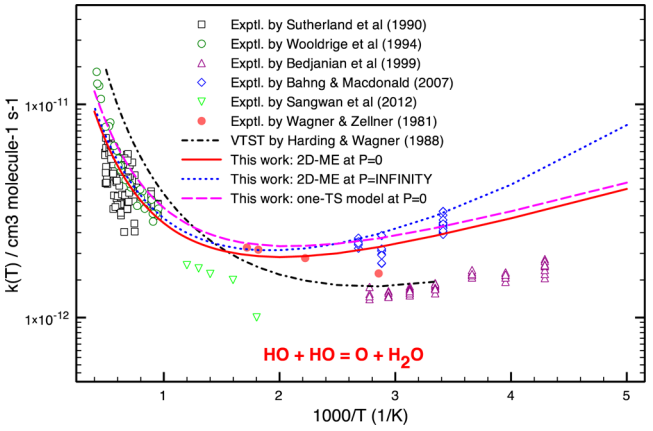

Figure 4. Calculated reaction rate constants as a function of temperature for the HO + HO = $O(^3P)$ + H_2O reaction. The experimental results and other theoretical values are given for comparison.

kcal/mol for the reaction DO + DO is higher than that of HO + HO, and (ii) second, the imaginary frequency is smaller, thus the contribution of tunneling is smaller. As a result, the minimum of reaction rate constant happens earlier, e.g., at lower temperature.

The one-TS model approach, eq 3, is also used to compute thermal rate constants. The one-TS model slightly overestimates $k(T)$ (by less than 15%) compared to the two-TS model (see Figures 2–4). This implies that the redissociation of PRC back to the initial reactants occurs more rapidly than the H-abstraction step to the products in this system.

The calculated reaction rate constant for the HO + HO reaction presented in Figure 4 shows a non-Arrhenius behavior and a strong curvature consistent with the experiments. At low temperatures, $k(T)$ decreases rapidly when increasing temperature, whereas at high temperatures, $k(T)$ increases sharply with the increase of temperature. So, the theoretical $k(T)$ curve has a minimum at about 500 K according to the experiments. As compared to the $k(T)$ calculated by Harding and Wagner[17] using the VTST/SCT approach, our values are larger at low temperatures, but become smaller at higher temperatures. The difference between the two approaches is, however, less than a factor of 2. Our predicted rate constants agree well with experiments at $T \geq 1000$ K in combustion (within 10%). At around room temperature, our calculations support the high

dx.doi.org/10.1021/jp312246q | J. Phys. Chem. A XXXX, XXX, XXX–XXX

values observed by Bahng and Macdonald,[8] rather than those measured by Bedjanian et al.[7] Note that Bedjanian et al. also measured the other two isotopic reactions and that our calculated $k(T)$ values agree with their measurements within 15%. It would then be surprising that we would overestimate the k(300 K) for the HO + HO reaction by a factor of 2. As mentioned in the Introduction section, with the use of experimental reaction rate constants measured by Bedjanian et al.[7] for the two reactions R3 and R4, a value of $(2.6 \pm 0.5) \times 10^{-12}$ cm^3 molecule^{-1} s^{-1} is estimated for reaction R1 at about room temperature under the ideal conditions. This value is in excellent agreement with 2.4×10^{-12} cm^3 molecule^{-1} s^{-1} calculated by us and also with $(2.7 \pm 0.9) \times 10^{-12}$ cm^3 molecule^{-1} s^{-1} observed by Bahng and Macdonald.[8] So, it is recommended that further experimental work should be done to further analyze the HO + HO rate constant.

Given that the calculated barriers in this work and also those reported elsewhere in the literature[17−19] are positive (i.e., TS1 always lies above the reactants), the reaction rate constants are assumed to be positive temperature dependent as usual. However, experimental results[9] and our calculations show an unusual behavior for the reaction rate constants, whose curve has a V-like shape (see Figure 4). So, it is important to understand what may cause this strange behavior. For the H-abstraction step from PRC to products, tunneling is expected to play some role. To estimate tunneling effects, we have rerun the simulation using eq 1, assuming that the reaction coordinate is completely separable from the other vibrations, which are perpendicular to the reaction coordinate. This assumption, which is one of the central premises in conventional TST,[44,45] is equivalent to setting all anharmonic constants X_{Fi} (i = 1 to $3N - 7$) and X_{FF} (which are related to the reaction coordinate) to be zero. In addition, the width of barrier along the reaction coordinate is set to infinity to ensure that there is no tunneling along the reaction path. In other words, the imaginary frequency (ω_F) needs to be set to near zero for the purpose of numerical calculations. This model is named conventional semiclassical TST (C-SCTST), which completely ignores multidimensional quantum mechanical tunneling but still includes coupled-vibration effects of the other orthogonal modes. The multidimensional quantum mechanical tunneling correction as a function of temperature is then computed as a ratio of SCTST $k(T)$ and C-SCTST $k(T)$, as given by eq 7:

$$\kappa(T) = k(T)_{\text{SCTST}}/k(T)_{\text{C-SCTST}} \quad (7)$$

The calculated values of $k_{\text{SCTST}}(T)$, $k_{\text{C-SCTST}}(T)$, and $\kappa(T)$ as functions of temperatures are plotted in Figure 5. Inspection of Figure 5 shows that $k_{\text{C-SCTST}}(T)$ without tunneling increases rapidly when increasing temperature as expected for the reaction with a positive barrier. In contrast, $\kappa(T)$ decreases sharply with the increase of temperature, for example, tunneling correction is 10.9 at 200 K, but reduces to 1.7 at 500 K and becomes negligible (1.06) at 1500 K. Because $k_{\text{SCTST}}(T)$ is a product of $k_{\text{C-SCTST}}(T)$ and $\kappa(T)$ (see eq 7), the unusual, non-Arrhenius behavior for the reaction rate constants is attributed to two coupled effects, namely, a positive barrier and quantum mechanical tunneling.

Tunneling corrections for the other two isotopic reactions were also calculated and were plotted in Figure 6. In general, tunneling decreases exponentially when temperature increases, and the order of tunneling factor arranging from the largest to the smallest for the three isotopic reactions is HO + HO, HO + DO, and DO + DO as expected. At 300 K, the tunneling

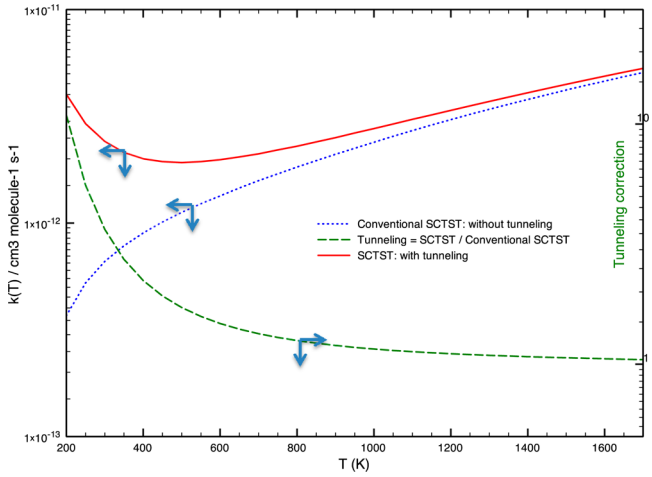

Figure 5. Calculated SCTST k(T), C-SCTST $k(T)$, and tunneling correction as a function of temperature for the HO + HO = O(^{3}P) + H_2O reaction.

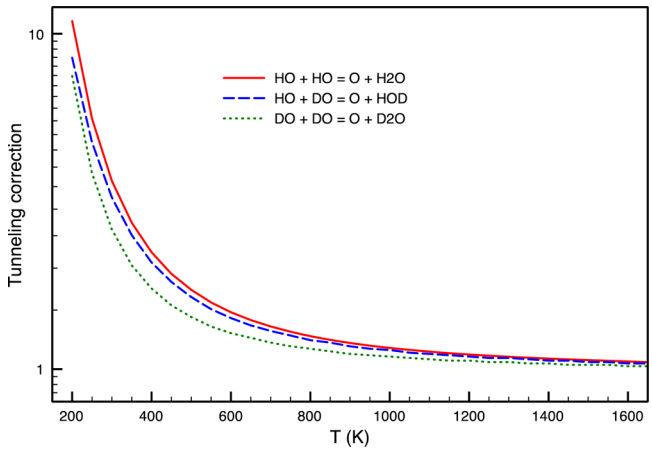

Figure 6. Tunneling correction as a function of temperature computed as a ratio of SCTST $k(T)$ and conventional SCTST $k(T)$ for three isotopic reactions.

correction for the HO + HO reaction is about 3.64. This means that, at 300 K, about 72% of the chemical reaction flux proceeds to the products by tunneling through the barrier. Therefore, tunneling is very important for this type of reaction and is responsible for the distinctly non-Arrhenius behavior for the observed reaction rate constants.

Thermal rate constants for the reverse reaction R-1 were also calculated with the forward reaction rate obtained above and the equilibrium constant of the reaction R1. The latter is calculated using the ro-vibrational parameters and the reaction enthalpy of −15.78 kcal/mol obtained in this work. The theoretical K_{eq} agrees well with the experimental ones,[46] better than 5%, in the temperature range of 700 to 2500 K. The calculated reaction rates in the temperature range of 700 to 2500 K (related to the application in combustion) are presented in Figure 7. As can be seen, our predictions are in excellent agreement with all experiments, better than 20%, at T > 1000 K although they seem to be slightly small at lower temperatures (T < 1000 K).

Does the Reaction Depend on Pressure? The title reaction is often assumed to be pressure independent.[4] To check this assumption, the reaction rate constants at the high-P limit as a function of temperature are calculated and presented

dx.doi.org/10.1021/jp312246q | J. Phys. Chem. A XXXX, XXX, XXX−XXX

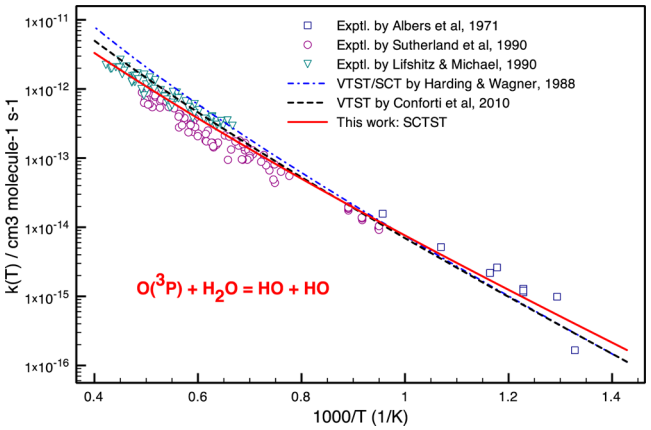

Figure 7. Calculated thermal rate constants as a function of temperature for the reverse reaction $O(^3P) + H_2O = HO + HO$. Experimental data and other theoretical work are given for comparison.

in Figure 4. As can be seen in Figure 4, there is a distinct difference between the calculated $k_{P=\infty}(T)$ and $k_{P=0}(T)$, especially at low temperatures. So, the reaction is predicted here to depend on pressure. As mentioned in the Computational Approach section, the difference between $k_{P=\infty}(T)$ and $k_{P=0}(T)$ is due to the tunneling reaction rate leading to products in the classical-forbidden region (e.g., see eqs 5c and 6). Consequently, the biggest deviation is found at the lowest temperature where tunneling plays the most important role. The difference between $k_{P=\infty}(T)$ and $k_{P=0}(T)$ decreases rapidly when temperature increases, for example, a factor of 2 is found at 200 K, but it becomes ca. 24% at 300 K and negligibly small at $T > 1000$ K. All measured values should fall in these two extremes. Except the experimental work of Sangwan et al.[4] who carried out their experiments at fairly high pressures ($P \leq 100$ atm), the other experimental work was done at low pressures ($P \leq 1$ atm), which is unquestionably close to the region of the low-P limit. In addition, the extreme condition of the high-P limit is hard to achieve experimentally. So, under the practical conditions in the atmosphere and combustion, the reaction is only slightly dependent on pressure and the difference between $k(T,P)$ and $k(T,P = 0)$ is very small, almost certainly within an uncertainty of the measurements. As a result, the 2D-ME model at the low-P limit makes perfect sense for this type of reaction. It should be noted that the dependence of pressure could, in principle, be tested by carrying out experiment under conditions of low temperatures (e.g., at 200 K) and high pressures (e.g., at 100 atm), where large divergences between $k_{P=\infty}(T)$ and $k_{P=0}(T)$ were found in the theoretical simulation.

What Are Possible Roles of Prereactive Complex? Reactions with the formation of a prereactive complex followed by its decomposition via an H-abstraction leading to products are often seen in the atmosphere and combustion.[9,10,31] So, it is of importance to understand possible roles of PRC. In terms of reaction mechanism and chemical kinetics, the PRC plays two key roles, namely, (i) first, PRC changes the shape of potential energy surface for the H-abstraction step, i.e., it makes the barrier larger and consequently reduces the width of barrier. This results in an increase of the reaction rate via tunneling; (ii) second, because of the existence of PRC, the reaction is slightly pressure dependent. This awaits to be verified by experiments in the future.

Sensitivity Analysis for Thermal Reaction Rate Constants. The calculated SCTST rate constants sensitively depend on several parameters, including barrier heights, rovibrational parameters, and anharmonic constants. Of these, the uncertainty in the barrier height is paramount. Given that the calculated barrier for TS1 in Figure 1 using HEAT is expected to have errors of up to 0.2 kcal/mol (see above), we shifted the energy of TS1 by this amount in order to carry out a simple sensitivity analysis. The thermal reaction rates calculated with and without the change of energy of TS1 are plotted in Figure 8. As can be seen in Figure 8, the sensitivity of the

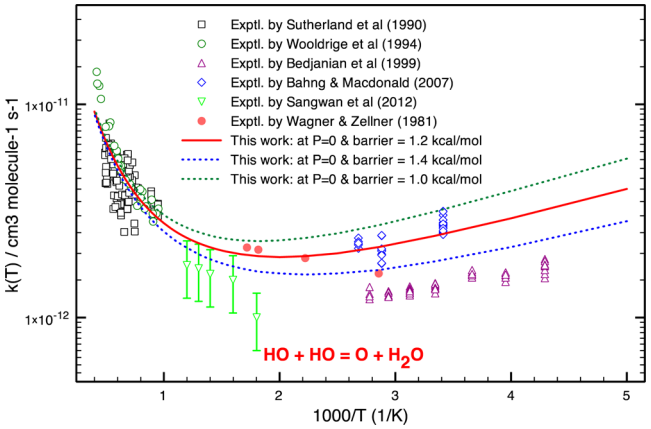

Figure 8. Calculated thermal rate constants as a function of temperature and a function of the position of TS1 for the $HO + HO = O(^3P) + H_2O$ reaction. The experimental results are presented for comparison.

results with respect to the TS1 barrier height is important at low temperatures but is reduced significantly at high temperatures. For example, at 200 K, a shift of TS1 by 0.2 kcal/mol alters the reaction rate by <40%, but the difference is <10% at 1000 K and becomes about 3% at 2500 K. Overall, it is gratifying to observe that most of the experimental values fall within the lower and upper limits of the theoretical reaction rate constants when the energy is varied as described, which suggests that the parameters calculated in this work are suitably accurate.

SUMMARY

The stationary points on triplet state potential energy surfaces for the $HO + HO = O(^3P) + H_2O$ reaction were computed using the HEAT protocol. The zero-point anharmonic vibration energies were obtained with second-order vibrational perturbation theory using the CCSD(T) method in combination with atomic natural orbital basis sets. The parameters obtained from quantum chemical calculations were then used as input data for chemical kinetics analysis using the SCTST/2D-ME approach under two extreme conditions of the low- and high-P limits in order to predict thermal rate constants for the title reaction and its H/D isotopologues. Some important results emerged from this study can be summarized as follows: (i) The HEAT calculation for the reaction enthalpy agrees excellently with the experimental one, within ±0.1 kcal/mol. The barrier height for the H-abstraction step leading to the products is predicted to be 1.2 ± 0.2 kcal/mol. (ii) The theoretical reaction rate constants for the forward and reverse reaction of $HO + HO = O(^3P) + H_2O$ and its two isotopic reactions are in very good agreement with the experiments,

dx.doi.org/10.1021/jp312246q | J. Phys. Chem. A XXXX, XXX, XXX−XXX

within 10 to 20%, over a wide temperature range. For the HO + HO = $O(^3P)$ + H_2O reaction, our calculated reaction rates support the high values observed by Bahng and Macdonald at around room temperature and are about twice those of Bedjanian et al. (iii) A non-Arrhenius behavior and a strong curvature for the reaction rate constant is found to be due to two coupled effects, namely, a positive (normal) barrier height and effects of quantum mechanical tunneling. Tunneling is very important, for example, even at 300 K, tunneling through the reaction barrier leading to the products contributes more than 70% of the total chemical reaction flux. (iv) Tunneling is also a main cause of a slight dependence of reaction rate on pressure. This awaits to be verified by experiments at low temperatures and high pressures in the future. Under the real conditions in the atmosphere and combustion, the chemical kinetic model at the low-*P* limit is sufficient. (v) Prereactive complex is found to play important roles in the reaction mechanism and chemical kinetics.

■ ASSOCIATED CONTENT

Supporting Information

Optimized geometries, rovibrational parameters, anharmonic constants, and energies for various species in the HO + HO = $O(^3P)$ + H_2O and its isotopic reaction are given. This material is available free of charge via the Internet at http://pubs.acs.org.

■ AUTHOR INFORMATION

Corresponding Author

*E-mail: jfstanton@mail.utexas.edu.

Notes

The authors declare no competing financial interest.

■ ACKNOWLEDGMENTS

J.F.S. and T.L.N. are supported by the Robert A. Welch Foundation (Grant F-1283) and the Department of Energy, Office of Basic Energy Sciences (Contract Number DE-FG02-07ER15884). We also thank Steven J. Klippenstein (Argonne National Laboratory) for comments on this work. T.L.N. appreciates Lawrence B. Harding (Argonne National Laboratory) for providing a copy of his excellent paper (ref 17).

■ REFERENCES

(1) Sellevag, S. R.; Georgievskii, Y.; Miller, J. A. Kinetics of the Gas-Phase Recombination Reaction of Hydroxyl Radicals to Form Hydrogen Peroxide. *J. Phys. Chem. A* **2009**, *113*, 4457−4467.

(2) Troe, J. The Thermal Dissociation/Recombination Reaction of Hydrogen Peroxide $H_2O_2(+M) \leftrightarrow 2OH(+M)$ III. Analysis and Representation of the Temperature and Pressure Dependence over Wide Ranges. *Combust. Flame* **2011**, *158*, 594−601.

(3) Fulle, D.; Hamann, H. F.; Hippler, H.; Troe, J. High Pressure Range of the Addition of HO to HO. III. Saturated Laser Induced Fluorescence Measurements between 200 and 700 K. *J. Chem. Phys.* **1996**, *105*, 1001−1006.

(4) Sangwan, M.; Chesnokov, E. N.; Krasnoperov, L. N. Reaction OH + OH Studied over the 298−834 K Temperature and 1−100 bar Pressure Ranges. *J. Phys. Chem. A* **2012**, *116*, 6282−6294.

(5) Glassman, I. *Combustion*, 2nd ed.; Academic Press: London, 1987.

(6) Gardiner, W. C., Jr. *Combustion Chemistry*; Springer-Verlag: New York, 1984.

(7) Bedjanian, Y.; Le Bras, G.; Poulet, G. Kinetic Study of OH + OH and OD + OD Reactions. *J. Phys. Chem. A* **1999**, *103*, 7017−7025.

(8) Bahng, M. K.; Macdonald, R. G. Determination of the Rate Constant for the $OH(X^2\Pi)$ + $OH(X^2\Pi)$ → $O(^3P)$ + H_2O Reaction over the Temperature Range 293−373 K. *J. Phys. Chem. A* **2007**, *111*, 3850−3861.

(9) Baulch, D. L.; Bowman, C. T.; Cobos, C. J.; Cox, R. A.; Just, T.; Kerr, J. A.; Pilling, M. J.; Stocker, D.; Troe, J.; Tsang, W.; Walker, R. W.; Warnatz, J. Evaluated Kinetic Data for Combustion Modeling: Supplement II. *J. Phys. Chem. Ref. Data* **2005**, *34*, 757−1397.

(10) Sander, S. P.; Abbatt, J.; Barker, J. R.; Burkholder, J. B.; Friedl, R. R.; Golden, D. M.; Huie, R. E.; Kolb, C. E.; Kurylo, M. J.; Moortgat, G. K.; Orkin, V. L.; Wine, P. H. *Chemical Kinetics and Photochemical Data for Use in Atmospheric Studies: Evaluation Number 17*; Jet Propulsion Laboratory: Pasadena, CA, 2011.

(11) Wooldridge, M. S.; Hanson, R. K.; Bowman, C. T. A Shock Tube Study of the OH + OH → H_2O + O Reaction. *Int. J. Chem. Kinet.* **1994**, *26*, 389−401.

(12) Deyerl, H. J.; Clements, T. G.; Khai Luong, A.; Continetti, R. E. Transition State Dynamics of the OH + OH → O + H_2O Reaction Studied by Dissociation Photodetachment of $H_2O_2^-$. *J. Chem. Phys.* **2001**, *115*, 6931−6940.

(13) Albers, E. A.; Hoyermann, K.; Wagner, H. G.; Wolfrum, J. Absolute Measurements of Rate Coefficients for the Reactions of H and O Atoms with H_2O_2 and H_2O. *13th Symp. (Int.) Combust.* **1971**, 81−88.

(14) Sun, H.; Li, Z. Rate Constant Measurement for the OH + OH → H_2O + O Reaction at 220−320 K using Discharge Flow/Mass Spectrometer/Resonance Fluorescence Technique. *Chem. Phys. Lett.* **2004**, *399*, 33−38.

(15) Lifshitz, A.; Michael, J. V. Rate Constants for the Reaction, O + H_2O → OH + OH over the Temperature Range, 1500−2400 K, by the Flash Photolysis-Shock Tube Technique: A Further Consideration of the Back Reaction. *23th Symp. (Int.) Combust.* **1990**, 59−67.

(16) Sutherland, J. W.; Patterson, P. M.; Klemm, R. B. Rate Constants for the Reaction, $O(^3P)$ + $H_2O \leftrightarrow$ OH + OH over the Temperature Range 1053 to 2033 K uisng Two Direct Techniques. *23th Symp. (Int.) Combust.* **1990**, 51−57.

(17) Harding, L. B.; Wagner, A. F. Theoretical Study of the Reaction Rates of OH + OH ↔ H_2O + O. *22nd Symp. (Int.) Combust.* **1988**, 983−989.

(18) Karkach, S. P.; Osherov, V. I. Ab Initio Analysis of the Transition States on the Lowest Triplet H_2O_2 Potential Surface. *J. Chem. Phys.* **1999**, *110*, 11918−11927.

(19) Conforti, P. F.; Braunstein, M.; Braams, B. J.; Bowman, J. M. Global Potential Energy Surfaces for $O(^3P)$ + $H_2O(^1A_1)$ Collisions. *J. Chem. Phys.* **2010**, *133*, 164312−10.

(20) Tajti, A.; Szalay, P. G.; Csaszar, A. G.; Kallay, M.; Gauss, J.; Valeev, E. F.; Flowers, B. A.; Vazquez, J.; Stanton, J. F. HEAT: High Accuracy Extrapolated Ab Initio Thermochemistry. *J. Chem. Phys.* **2004**, *121*, 11599−11613.

(21) Bomble, Y. J.; Vazquez, J.; Kallay, M.; Michauk, C.; Szalay, P. G.; Csaszar, A. G.; Gauss, J.; Stanton, J. F. High-Accuracy Extrapolated Ab Initio Thermochemistry. II. Minor Improvements to the Protocol and a Vital Simplification. *J. Chem. Phys.* **2006**, *125*, 064108−8.

(22) Harding, M. E.; Vazquez, J.; Ruscic, B.; Wilson, A. K.; Gauss, J.; Stanton, J. F. High-Accuracy Extrapolated Ab Initio Thermochemistry. III. Additional Improvements and Overview. *J. Chem. Phys.* **2008**, *128*, 114111−15.

(23) Nguyen, T. L.; Stanton, J. F.; Barker, J. R. A Practical Implementation of Semi-Classical Transition State Theory for Polyatomics. *Chem. Phys. Lett.* **2010**, *499*, 9−15.

(24) Miller, W. H. Semiclassical Theory for Non-Separable Systems-Construction of Good Action-Angle Variables for Reaction-Rate Constants. *Faraday Discuss.* **1977**, *62*, 40−46.

(25) Miller, W. H.; Hernandez, R.; Handy, N. C.; Jayatilaka, D.; Willets, A. Ab Initio Calculation of Anharmonic Constants for a Transition-State, with Application to Semiclassical Transition-State Tunneling Probabilities. *Chem. Phys. Lett.* **1990**, *172*, 62−68.

(26) Nguyen, T. L.; Stanton, J. F.; Barker, J. R. Ab Initio Reaction Rate Constants Computed Uisng Semiclassical Transition-State Theory: HO + H_2 → H_2O + H and Isotopologues. *J. Phys. Chem. A* **2011**, *115*, 5118−5126.

(27) Ruscic, B.; Boggs, J. E.; Burcat, A.; Csaszar, A. G.; Demaison, J.; Janoschek, R.; Martin, J. L.; Morton, M. L.; Rossi, M. J.; Stanton, J. F.; Szalay, P. G.; Westmoreland, P. R.; Zabel, F.; Berces, T. IUPAC Critical Evaluation of Themochemical Properties of Selected Radicals. Part I. *J. Phys. Chem. Ref. Data* **2005**, *34*, 573−656. All ATcT results are based on the Core (Argone) Thermochemical Network, Version 1.064, 2007.
(28) Almlof, J.; Taylor, P. R. General Constraction of Gaussian-Basis Sets. 1. Atomic Natural Orbitals for 1st-Row and 2nd-Row Atoms. *J. Chem. Phys.* **1987**, *86*, 4070−4077.
(29) Almlof, J.; Taylor, P. R. General Constraction of Gaussian-Basis Sets. 2. Atomic Natural Orbitals and the Calculation of Atomic and Molecular-Properties. *J. Chem. Phys.* **1990**, *92*, 551−560.
(30) Stanton, J. F.; Gauss, J.; Harding, M. E.; Szalay, P. G.; et al. *CFOUR*, Coupled-Cluster Techniques for Computational Chemistry; University of Texas at Austin: Austin, TX, 2009.
(31) Atkinson, R.; Baulch, D. L.; Cox, R. A.; Crowley, J. N.; Hampson, R. F.; Hynes, R. G.; Jenkin, M. E.; Rossi, M. J.; Troe, J. Evaluated Kinetic and Photochemical Data for Atmospheric Chemistry: Volume III-Gas Phase Reactions of Inorganic Halogens. *Atmos. Chem. Phys.* **2007**, *7*, 981−1191.
(32) Barker, J. R.; Ortiz, N. F.; Preses, J. M.; Lohr, L. L.; Maranzana, A.; Stimac, P. J.; Nguyen, T. L.; Kumar, T. J. D. *MultiWell*; University of Michigan: Ann Arbor, MI, 2011; see http://aoss.engin.umich.edu/multiwell/.
(33) Miller, W. H. Unified Statistical-Model for Complex and Direct Reaction-Mechanisms. *J. Chem. Phys.* **1976**, *65*, 2216−2223.
(34) Troe, J. The Polanyi Lecture: The Colorful World of Complex-Forming Bimolecular Reactions. *J. Chem. Soc. Faraday Trans.* **1994**, *90*, 2303−2317.
(35) Peeters, J.; Vereecken, L. *International Gas Kinetics Conference, GK2006*, Orléans, France, July 22−27, 2006.
(36) Greenwald, E. E.; North, S. W.; Georgievskii, Y.; Klippenstein, S. J. A Two Transition State Model for Radical-Molecule Reactions: A Case Study of the Addition of OH to C_2H_4. *J. Phys. Chem. A* **2005**, *109*, 6031−6044.
(37) Horiuti, J. On the Statistical Mechanical Treatment of the Absolute Rate of Chemical Reaction. *Bull. Chem. Soc. Jpn.* **1938**, *13*, 210.
(38) Truhlar, D. G.; Garrett, B. C. Resonance State Approach to Quantum-Mechanical Variational Transition-State Theory. *J. Phys. Chem.* **1992**, *96*, 6515−6518.
(39) Beyer, T.; Swinehart, D. F. Number of Multiply-Restricted Partitions. *Commyn. Assoc. Comput. Mach.* **1973**, *16*, 379−379.
(40) Stein, S. E.; Rabinovitch, B. S. Accurate Evaluation of Internal Energy-Level Sums and Densities Including Anharmonic Oscillators and Hindered Rotors. *J. Chem. Phys.* **1973**, *58*, 2438−2445.
(41) Truhlar, D. G.; Garrett, B. C.; Klippenstein, S. J. Current Status of Transition-State Theory. *J. Phys. Chem.* **1996**, *100*, 12771−12800.
(42) Singleton, D. L.; Cvetanovic, R. J. Temperature-Dependence of Reactions of Oxygen-Atoms with Olefins. *J. Am. Chem. Soc.* **1976**, 6812−6819.
(43) Alvarez-Idaboy, J. R.; Mora-Diez, N.; Vivier-Bunge, A. A Quantum Chemical and Classical Transition State Theory Explanation of Negative Activation Energies in OH Addition to Substituted Ethenes. *J. Am. Chem. Soc.* **2000**, *112*, 3715−3720.
(44) Eyring, H. The Activated Complex in Chemical Reactions. *J. Chem. Phys.* **1935**, *3*, 107−115.
(45) Evans, M. G.; Polanyi, M. Some Applications of the Transition State Method to the Calculation of Reaction Velocities, especially in Solution. *Trans. Faraday Soc.* **1935**, *31*, 875−893.
(46) Chase, M. W. NIST-JANAF Thermochemical Tables, 4th ed. *J. Phys. Chem. Ref. Data* **1998**, *9*, 1−1951.